A prognostic model constructed by CTHRC1 and LRFN4 in Stomach adenocarcinoma by Bioinformatics Analysis

Songling Han
Zhejiang University
Wei Zhu
Zhejiang University
Qijie Guan
Zhejiang University
Zhuoheng Zhong
Zhejiang University
Ruoke Zhao
Zhejiang University
Hangming Xiong
Zhejiang University
Hongwei Fu
Zhejiang University
Xingjiang Hu (huxingjiang@zju.edu.cn)
Zhejiang University School of Medicine First Affiliated Hospital
Jingkui Tian
Zhejiang University

Research

Keywords: Stomach adenocarcinoma, Bioinformatics analysis, Differentially expressed genes, Biomarker, Gene Expression Omnibus

Posted Date: August 7th, 2020

DOI: https://doi.org/10.21203/rs.3.rs-52939/v1

Abstract

Background

Stomach adenocarcinoma (STAD) is the most common histological type of stomach cancer, which causes a considerable number of deaths worldwide. This study specifically aimed to identify potential biomarkers and reveal the underlying molecular mechanisms.

Methods

Gene expression profiles microarray data were downloaded from the Gene Expression Omnibus (GEO) database. The 'limma' R package was used to screen the differentially expressed genes (DEGs) between STAD and matched normal tissues. The Database for Annotation, Visualization, and Integrated Discovery (DAVID) was used for function enrichment analyses of DEGs. The data of STAD cases with both RNA sequencing and clinical information of The Cancer Genome Atlas (TCGA) were obtained from Genomic Data Commons (GDC) data portal. Survival curves were analyzed by the Kaplan-Meier method, univariate Cox regression analysis and multivariate Cox regression were performed using 'survival' package. CIBERSORT algorithm used approach to characterize the 22 human immune cell composition. Gene expression profiles microarray data and clinical information were downloaded from GEO database to validate prognostic model.

Results

Three public datasets including 90 STAD patients and 43 healthy controls were used and 44 genes were differentially expressed in all three datasets. These genes were primarily implicated in biological processes including cell adhesion, wound healing and extracellular matrix organization. Seven out of 44 genes showed significant survival differences based on their expression differences. *CTHRC1* and *LRFN4* were eventually used to constructed risk score and prognostic model by univariate Cox regression and stepwise multivariate Cox regression in The Cancer Genome Atlas (TCGA)-STAD dataset. The group having high risk scores and the group having low risk scores had significant differences in the infiltration level of multiple immune cells including CD4 memory resting T cells, M2 macrophages, memory B cells, resting dendritic cells, eosinophils, and gamma delta T cells. Multivariate Cox regression analyses indicated that the risk score was an independent predictor after adjusting for age, sex, and tumor stage. At last, the model was verified and evaluated by another independent dataset and showed a good classification effect.

Conclusions

The present study constructed the prognostic model by expression of *CTHRC1* and *LRFN4* for the first time via comprehensive bioinformatics analysis, which may provide clinical guidance and potential therapeutic targets for STAD.

Background

Stomach adenocarcinoma (STAD), the most common histological type (~ 95%) of malignancy originating in the stomach, imposes a considerable global health burden [1]. However, there are no sensitive and specific diagnostic markers for early diagnosis of STAD. Although several drugs, such as trastuzumab, ramucirumab and immune checkpoint inhibitors, have been used for the treatment of STAD in the clinic, the survival rates of patients in advanced stages are low [2–4]. Therefore, identifying novel diagnostic biomarkers and developing therapeutic medicines for STAD are necessary.

Over the past decades, the development of high-throughput sequencing has produced large-scale biological data, and it has been an effective tool for discovering promising biomarkers for cancer [5]. Many potential therapeutic targets, including *AFP*, *EGFR* and *HER2*, have been explored by bioinformatic analysis [6–8]. Bioinformatic analysis has also played an important role in the potential biomarkers discovery for the diagnosis and treatment of stomach-related cancer: *COL4A1* is a therapeutic target for recurrent gastric carcinoma; *FN1*, *SERPINE1*, and *SPARC* significantly predict poor prognosis of STAD; and nine hub genes have been identified to be strongly correlated with the pathogenesis of gastric cancer [9–11]. Despite the partial success of the above studies, there were two weaknesses. First, most of the studies focused on gene expressions and clinical data analyses, while the molecular mechanism of STAD was not extensively elucidated. Second, several biomarkers were revealed. Moreover, the approaches for treating STAD were not provided, which could possibly make clinical treatment difficult.

In the present study, we analyzed the mRNA expression profiles of STAD from Gene Expression Omnibus (GEO) database and obtained the differentially expressed genes (DEGs). Then, gene ontology (GO) analyses were further conducted to analyze the main biological functions modulated by the DEGs. By survival information was analyzed in patients with STAD from The Cancer Genome Atlas (TCGA), the candidate genes closely related to survival rate of patients were identified. Cox analysis was used to further screening mRNAs correlated with survival rates and constructed prognostic risk assessment model. In order to find the cause of the differences in patient survival, we gourped the immune cell infiltration in the high- and low-risk groups, and analyzed the relationship between the mRNAs and immune cell infiltration. Finally, we used another independent data set to verify the prognostic effect of our model. Through this research, we aimed to identify high-quality biomarkers for STAD and provide reasonable results for further elucidation of the molecular mechanism of STAD.

Materials And Methods

Data collection and screening of DEGs. Gene expression profiles microarray data (GSE118916 of 15 STAD and 15 healthy tissues, GSE13861 of 65 STAD and 19 healthy tissues, GSE103236 of 10 STAD and

9 healthy tissues) were downloaded from the Gene Expression Omnibus (GEO) database (https://www.ncbi.nlm.nih.gov/geo/). The 'limma' R package was used to screen the DEGs between STAD and matched normal tissues [12]. Adjusted p-value < 0.05 and |log2 fold change (FC)| > 1 were set as the thresholds for DEG identification.

GO enrichment analyses. The Database for Annotation, Visualization, and Integrated Discovery (DAVID, https://david.ncifcrf.gov/) was used for biological process (BP), cellular component (CC) and molecular function (MF) enrichment analyses of DEGs [13]. P-value < 0.05 was used to screen statistically significant terms.

TCGA data analysis and survival analysis of DEGs. The data of STAD cases with both RNA sequencing and clinical information of TCGA were obtained from Genomic Data Commons (GDC) data portal (https://portal.gdc.cancer.gov/). We deleted cases with missing clinical information and therefore retained 370 cases. The mRNA high-level and low-level grouping was based on the median expression value of the mRNA, Survival curves were analyzed by the Kaplan-Meier method [14]. P-value < 0.05 was considered statistically significant.

Grouping of Samples and Construction of Prognostic Model. We used R 3.6.2 with 'survival' package to univariate Cox regression analysis and multivariate Cox regression. In order to reduce the number of mRNAs with similar expressions, mRNAs with p-value < 0.05 of univariate Cox regression were subjected to a stepwise multivariate Cox regression to construct the prognostic model. This model was used to evaluate the survival prognosis of patients in TCGA-STAD datasets using Kaplan-Meier curve, and log-rank test according to median value grouping of risk score.

Inference of infiltrating cells in the TME. We used the CIBERSORT algorithm and the LM22 gene signature, which is a widely used approach to characterize the 22 human immune cell composition, including B cells, T cells, nature killer cells and macrophages[15]. After uploading the gene expression data with standard annotation on to the CIBERSORT web portal (http://cibersort.stanford.edu/), the algorithm ran under LM22 signature and 1,000 permutations.

Validation and Evaluation of Prognostic Model. Gene expression profiles microarray data (GSE84437 of 443 gastric cancer cases) were downloaded from GEO database to validate our prognostic model. The prognostic model was used to evaluate the survival prognosis of each patients in GSE84437 datasets using Kaplan-Meier curve, and log-rank test according to median value grouping of risk scores.

Statistical analysis. The present study used Mann-Whitney U tests (also called the Wilcoxon rank-sum test) statistically analyzing the gene expression and immune infiltration of two groups. A threshold of $p < 0.05$ was considered statistically significant. The gene expression correlation and correlation between immune infiltration and gene expression was accessed by Pearson's R and statistical significance. The absolute value of R greater than 0.1 was considered to be relevant and p-value < 0.05 was considered statistically significant. Gene expression data were processed by plus 1 and then take the log2 value.

Results

Identification of DEGs. A total of 3,860 DEGs were screened from the GSE118916 dataset. In addition, 550 and 463 DEGs were selected from the GSE13861 and GSE103236 datasets, respectively. Volcano plots were plotted to present the distribution of DEGs between OSCC and normal samples in each dataset (Fig. 1A-C). After the combination, a total of 44 DEGs with adjusted p-value < 0.05 and |log2 fold change (FC)| > 1 were screened out at the intersection of the three datasets.

Functional and pathway enrichment analyses of the DEGs. To reveal the biological functions of the DEGs, GO enrichment analysis was conducted with DAVID. Regarding molecular function, the GO analysis results showed that the DEGs were mainly enriched in terms related to extracellular matrix binding and cytokine activity. These DEGs were involved in cell adhesion, wound healing and extracellular matrix organization biological processes. For cellular components, the DEGs were enriched in extracellular regions, including the proteinaceous extracellular matrix, extracellular region and extracellular space (Fig. 2).

Survival analysis of DEGs.

To further evaluate the prognostic value of the 45 DEGs, the clinical data of patients with STAD were downloaded from the TCGA database. The overall survival of patients with STAD based on the high and low expression of DEGs, was then obtained using Kaplan–Meier plotters. The results indicated that the high expression of *DPT*, *COL5A2*, *CTHRC1* and low expression of *ECT2*, *LRFN4* was associated with poor overall survival in patients with STAD (Fig. 3). In short, we found 5 genes that were significantly related to the prognosis of patients with STAD.

Construction and Evaluation of Prognostic Model.

The univariate Cox regression analysis displayed that of 5 mRNAs were found to be associated with overall survival in TCGA-STAD dataset (N = 370). Three mRNAs of p-value < 0.05 were selected for further analysis (Table 1). Two (*LRFN4*, *CTHRC1*) of three mRNAs screend out by stepwise multivariate Cox regression analysis (Fig. 4A). Then, the prognostic model was constructed by expression of *LRFN4* and *CTHRC1* and its coefficient in multivariate Cox regression as follows: risk score = (-0.20788 × expression of *LRFN4*) + (0.18741 × expression of *CTHRC1*). According to the median value of risk scores, patients were divided into the high-risk group and the low-risk group, while high-risk group has worse prognosis (Fig. 4B). Delete data with missing age, sex and tumor stage information and keep 344 samples for the next analysis. Multivariate Cox regression analyses also revealed that the risk score was an independent predictor of survival in TCGA datasets, after adjusting for age (< 60 vs. ≥60), sex (male vs. female), and tumor stage (I and II vs. III and IV) (Fig. 5).

Immune microenvironment analysis.

The difference of tumor infiltrating immune cell composition between the high-risk group and the low-risk group was analyzed by CIBERSORT. The infiltration level of eight immune cells was significant between

the two groups, including CD4 memory resting T cells, M2 macrophages, memory B cells, resting dendritic cells, eosinophils, gamma delta T cells (Fig. 6). We also explored the relationships between these six immune cells and the expression of two genes include *LRFN4* and *CTHRC1*. The result showed that infiltration levels of CD4 memory resting T cells, memory B cells, eosinophils and gamma delta T cells were significantly correlated with expression levels of *LRFN4* and infiltration level of CD4 memory resting T cells, memory B cells and M2 macrophages were significantly related with expression of *CTHRC1* (Fig. 7).

Evaluation of Prognostic Model for Over Survival in GEO dataset

We evaluated our model by GSE84437 dataset download from GEO database (N = 443). The expression of *CTHRC1* was higher in the high-risk group and the expression of *LRFN4* was higher in the low-risk group in TCGA-STAD dataset (Fig. 8A, B). The expression of *CTHRC1* and *LRFN4* showed the same expression pattern in the GSE84437 dataset (Fig. 9A, B). In addition, the risk score of each patient was calculate by the prognostic model proposed above and divide the patients of GSE84437 dataset into high-risk group and low-risk group based on the median risk score. Survival analysis results showed that patients had a worse prognosis in the high-risk group (Fig. 9C).

Discussion

In the present study, 44 DEGs were identified between STAD and healthy samples from three datasets. To better clarify the functions of DEGs, we further performed functional enrichment analysis. The proteins translated by DEGs were mainly located in extracellular regions and these genes were primarily implicated in tumor-related biological processes such as cell adhesion, wound healing and extracellular matrix organization [16–18].

Then, seven candidate genes (*DPT*, *ECT2*, *COL5A2*, *CTHRC1*, and *LRFN4*) that were closely related to the survival rate of STAD patients were identified by analyzing the total survival information from STAD patients in TCGA program. Based on the results of univariate Cox regression and stepwise multivariate Cox regression in TCGA-STAD dataset, *CTHRC1* and *LRFN4* were eventually used to constructed risk score and prognostic model. Kaplan-Meier curves showed that the high-risk group had an obviously poorer overall survival compared to the low-risk group in the three groups. In addition, multivariate Cox regression analyses indicated that the risk score was an independent predictor of survival in TCGA datasets, after adjusting for age, sex, and tumor stage.

CTHRC1 encodes a protein that may play a role in the cellular response to arterial injury through involvement in vascular remodeling [19]. Previous studies had shown that *CTHRC1* promoted tumor cell progression and might play a key role in the invasion and metastasis of cervical carcinoma, cervical squamous cell carcinoma and colorectal cancer [20–22]. In addition, *CTHRC1* promotes M2-like

macrophage recruitment and myometrial invasion in endometrial carcinoma by integrin-Akt signaling pathway [23], which indicated that *CTHRC1* might be a biomarker for tumor immunotherapy.

LRFN4 encodes leucine-rich repeat and fibronectin type III domain-containing 4, belongs to the superfamily of leucine-rich repeat-containing adhesion molecules [24]. In a previous study, *LRFN4* was highly expressed in tumor cells, which is consistent with our analysis results (FIG S1) [25]. However, this study showed that high expression of *LRFN4* is associated with poor prognosis, which contradicts our findings (Fig. 3C). Due to the lack of researches on the relationship of *LRFN4* and cancer, the correlations between *LRFN4* and cancer need to be verified.

Next, immune cell infiltration analysis showed that eight immune cells have difference in the high-risk group and the low-risk group. Some studies have revealed the important role of these cells in cancer. For example, M2 macrophages were suppressors of anti-tumor immunity and gamma delta T cells were significantly correlated with an increased risk of death in pancreatic ductal adenocarcinoma [26, 27]. Moreover, infiltration level of three immune cells including CD4 memory resting T cells, memory B cells and M2 macrophages were significantly correlated with expression of *CTHRC1* and four immune cells contain CD4 memory resting T cells, memory B cells, eosinophils and gamma delta T cells were significantly related with expression of *LRFN4*. These results indicated that the expression of *CTHRC1* and *LRFN4* may affect tumor growth, metastasis and invasion through these immune cells, further affecting the prognosis of patients.

In the last, we downloaded a data set (GSE84437) including 443 patients' clinical and gene expression information from GEO database. Based on the median risk score derived from the prognostic model, 443 patients were divided into the high-risk group and the low-risk group. Survival analysis showed that survival time of patients in the high-risk group was significantly lower than that in the low-risk group. And in both the prognostic model and the verifying model, *CTHRC1* was higher expressed in the high-risk group, and *LRFN4* was lower expressed in the high-risk group. These results indicated that our model performed well in different data sets and had good clinical application prospects.

Despite all of these studies, our research still included some limitations: (a) The prognostic model is based on the expression of genes in the tissue and based on the expression of genes and proteins in the blood have more convenience in clinical application; (b) The prognostic effect of *CTHRC1* and *LRFN4* had been manifested, but the specific role played in STAD still needs further clarification. Therefore, these will also be the focus of our next study.

In conclusion, we constructed a new predictive model of mRNA prognosis through mRNA expression profiling, the model was verified and evaluated by another independent dataset. In addition, we analyzed the possible causes of the difference in prognosis from the perspective of immune microenvironment. However, this is just a study based on the online database using bioinformatics. We hope that there will be numerous of experiments to verify the feasibility of this prognostic model in the future and provide a reliable predictor and therapeutic target for STAD patients.

Declarations

Ethics approval and consent to participate

Not applicable.

Consent for publication

Not applicable.

Availability of data and materials

The datasets used and/or analyzed during the present study are available from the corresponding author on reasonable request.

Competing interests

The authors declare that they have no competing interests.

Funding

This work was supported by National Science and Technology Major Project of China (Grant No. 2017ZX09301007) and Zhejiang Provincial Science and Technology Planning Project (Grant No. 2016C04005).

Authors' contributions

XJH, JKT and HWF conceived and designed the study, and the experiments were performed by SLH, WZ, HMX and RKZ analyzed the data and wrote the manuscript. The original text was drafted and modified by ZHZ and QJG. All authors read and approved the final manuscript.

Acknowledgments

Not applicable.

References

1. Ajani JA, Lee J, Sano T, Janjigian YY, Fan D, Song S. Gastric adenocarcinoma. Nat Rev Dis Prim. 2017;3:17036.

2. Bang YJ, Van Cutsem E, Feyereislova A, Chung HC, Shen L, Sawaki A, et al. Trastuzumab in combination with chemotherapy versus chemotherapy alone for treatment of HER2-positive advanced gastric or gastro-oesophageal junction cancer (ToGA): A phase 3, open-label, randomised controlled trial. Lancet Elsevier Ltd. 2010;376:687–97.
3. Fuchs CS, Tomasek J, Yong CJ, Dumitru F, Passalacqua R, Goswami C, et al. Ramucirumab monotherapy for previously treated advanced gastric or gastro-oesophageal junction adenocarcinoma (REGARD): An international, randomised, multicentre, placebo-controlled, phase 3 trial. Lancet. 2014;383:31–9.
4. Fuchs CS, Doi T, Jang RW, Muro K, Satoh T, Machado M, et al. Safety and efficacy of pembrolizumab monotherapy in patients with previously treated advanced gastric and gastroesophageal junction cancer: Phase 2 clinical KEYNOTE-059 trial. JAMA Oncol. 2018;4:1–8.
5. Jiang P, Liu XS. Big data mining yields novel insights on cancer. Nat Genet. 2015;47:103–4.
6. Tateishi R, Yoshida H, Matsuyama Y, Mine N, Kondo Y, Omata M. Diagnostic accuracy of tumor markers for hepatocellular carcinoma: A systematic review. Hepatol Int. 2008;2:17–30.
7. Vizoso M, Ferreira HJ, Lopez-Serra P, Carmona FJ, Martínez-Cardús A, Girotti MR, et al. Epigenetic activation of a cryptic TBC1D16 transcript enhances melanoma progression by targeting EGFR. Nat Med. 2015;21:741–50.
8. Alix-Panabières C, Pantel K. Clinical applications of circulating tumor cells and circulating tumor DNA as liquid biopsy. Cancer Discov. 2016;6:479–91.
9. Li DF, Wang NN, Chang X, Wang SL, Wang LS, Yao J, et al. Bioinformatics analysis suggests that COL4A1 may play an important role in gastric carcinoma recurrence. J Dig Dis. 2019;391–400.
10. Li L, Zhu Z, Zhao Y, Zhang Q, Wu X, Miao B, et al. FN1, SPARC, and SERPINE1 are highly expressed and significantly related to a poor prognosis of gastric adenocarcinoma revealed by microarray and bioinformatics. Sci Rep. 2019;9:1–9.
11. Liu X, Wu J, Zhang D, Bing Z, Tian J, Ni M, et al. Identification of potential key genes associated with the pathogenesis and prognosis of gastric cancer based on integrated bioinformatics analysis. Front Genet. 2018;9:1–14.
12. Ritchie ME, Phipson B, Wu D, Hu Y, Law CW, Shi W, et al. Limma powers differential expression analyses for RNA-sequencing and microarray studies. Nucleic Acids Res. 2015;43:e47.
13. Huang DW, Sherman BT, Tan Q, Collins JR, Alvord WG, Roayaei J, et al. The DAVID Gene Functional Classification Tool: A novel biological module-centric algorithm to functionally analyze large gene lists. Genome Biol. 2007;8.
14. Guyot P, Ades AE, Ouwens MJNM, Welton NJ. Enhanced secondary analysis of survival data: Reconstructing the data from published Kaplan-Meier survival curves. BMC Med Res Methodol. 2012;12.
15. Yoshihara K, Shahmoradgoli M, Martínez E, Vegesna R, Kim H, Torres-Garcia W, et al. Inferring tumour purity and stromal and immune cell admixture from expression data. Nat Commun. 2013;4.

16. Alfarsi LH, El Ansari R, Craze ML, Masisi BK, Ellis IO, Rakha EA, et al. PPFIA1 expression associates with poor response to endocrine treatment in luminal breast cancer. BMC Cancer BMC Cancer. 2020;20:1–8.
17. Yu Z, Wang Y, Jiang Y, zhang, Ma S, jie, Zhong Q, Wan Y yuan, et al. NID2 can serve as a potential prognosis prediction biomarker and promotes the invasion and migration of gastric cancer. Pathol Res Pract. Elsevier; 2019;215:152553.
18. Liao X, Bu Y, Xu Z, Jia F, Chang F, Liang J, et al. WISP1 Predicts Clinical Prognosis and Is Associated With Tumor Purity, Immunocyte Infiltration, and Macrophage M2 Polarization in Pan-Cancer. Front Genet. 2020;11:1–11.
19. Pyagay P, Heroult M, Wang Q, Lehnert W, Belden J, Liaw L, et al. Collagen triple helix repeat containing 1, a novel secreted protein in injured and diseased arteries, inhibits collagen expression and promotes cell migration. Circ Res. 2005;96:261–8.
20. Zheng M, Zhou Q, Liu X, Wang C, Liu G. CTHRC1 overexpression promotes cervical carcinoma progression by activating the Wnt/PCP signaling pathway. Oncol Rep. 2019;41:1531–8.
21. Li N, Chen L, Liu C, Jiang Y, Rong J. Elevated CTHRC1 expression is an indicator for poor prognosis and lymph node metastasis in cervical squamous cell carcinoma. Hum Pathol. 2019;85:235–41.
22. Ni S, Ren F, Xu M, Tan C, Weng W, Huang Z, et al. CTHRC1 overexpression predicts poor survival and enhances epithelial-mesenchymal transition in colorectal cancer. Cancer Med. 2018;7:5643–54.
23. Li LY, Yin KM, Bai YH, Zhang ZG, Di W, Zhang S. CTHRC1 promotes M2-like macrophage recruitment and myometrial invasion in endometrial carcinoma by integrin-Akt signaling pathway. Clin Exp Metastasis Springer Netherlands. 2019;36:351–63.
24. Nam J, Mah W, Kim E. The SALM/Lrfn family of leucine-rich repeat-containing cell adhesion molecules. Semin Cell Dev Biol Elsevier Ltd. 2011;22:492–8.
25. Liu Y, Chen X, Chen X, Yang X, Song Q, Wu H. High SALM3 expression in tumor cells and fibroblasts is correlated with poor prognosis in gastric cancer patients. Dis Markers. 2019;2019.
26. Pritchard A, Tousif S, Wang Y, Hough K, Khan S, Strenkowski J, et al. Lung Tumor Cell-Derived Exosomes Promote M2 Macrophage Polarization. Cells. 2020;9.
27. Xu C, Sui S, Shang Y, Yu Z, Han J, Zhang G, et al. The landscape of immune cell infiltration and its clinical implications of pancreatic ductal adenocarcinoma. J Adv Res Cairo University. 2020;24:139–48.

Tables

Table 1. Prognostic value detection of the five genes via univariate survival-related analysis in patients with STAD of TCGA cohort.

Gene	HR	Low	High	p-Value
LRFN4	0.822269	0.693798	0.974528	0.023968
COL5A2	1.231122	1.060467	1.42924	0.006312
CTHRC1	1.201508	1.062042	1.359289	0.003544
ECT2	0.890144	0.759215	1.043652	0.151683
DPT	1.082031	0.968893	1.208381	0.161769

Figures

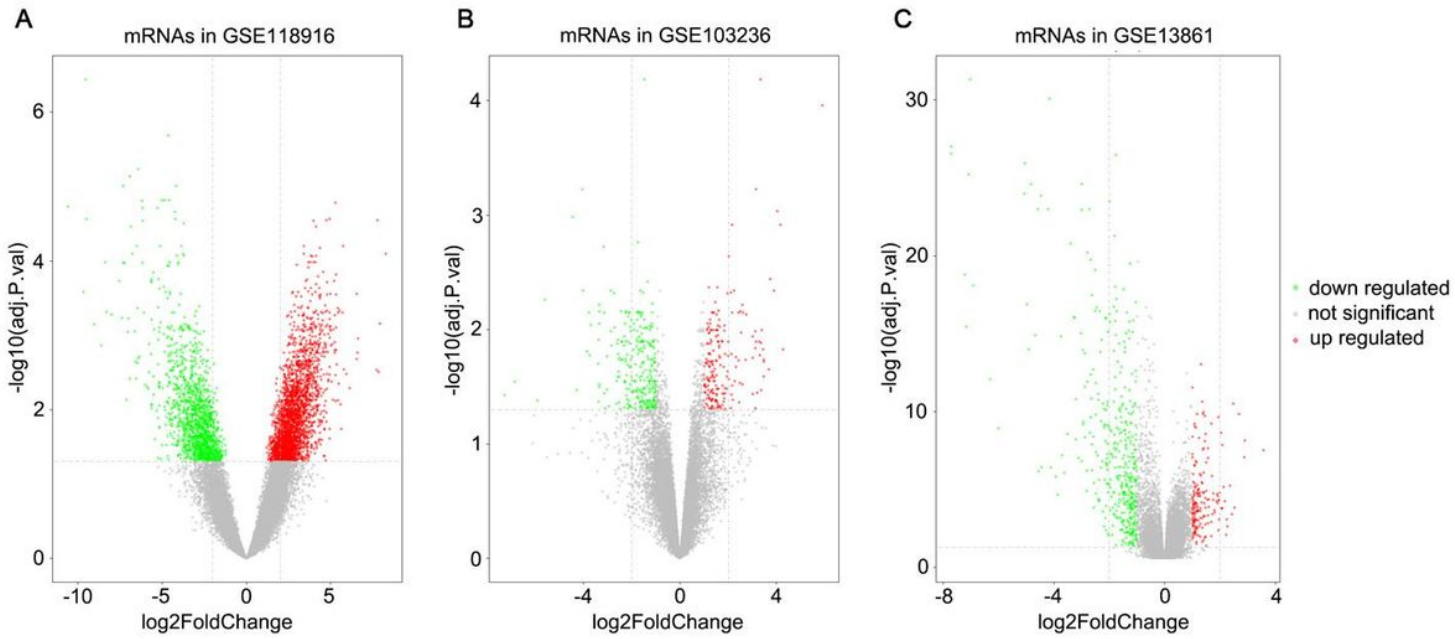

Figure 1

Volcano plots of DEGs in the three GEO datasets. Each dot represents a gene, green represents down-regulation and red represents up-regulation. (A) DEGs of GSE118916 dataset. (B) DEGs of GSE103036 dataset. (C) DEGs of GSE13861 dataset.

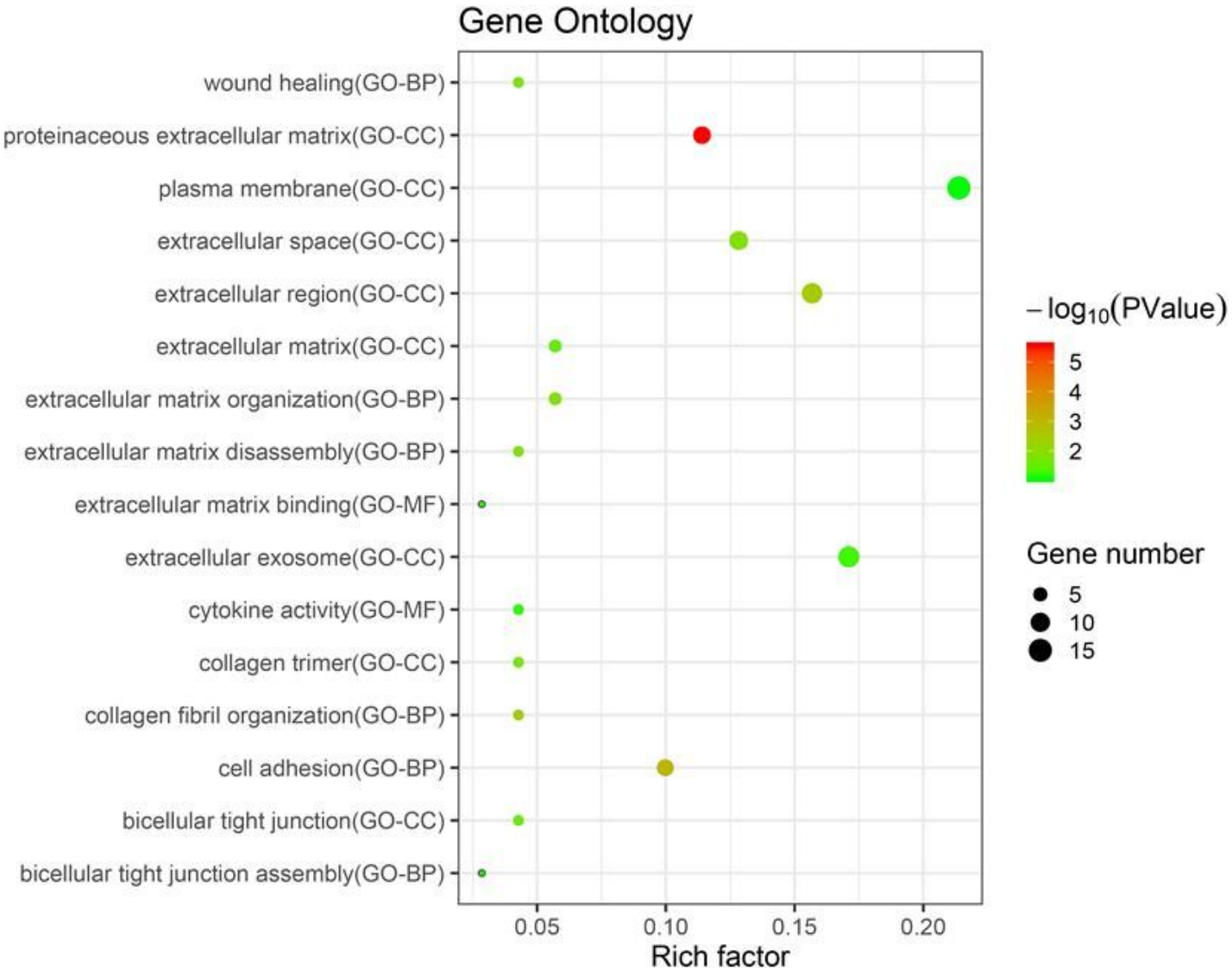

Figure 2

Statistics of functional enrichment. CC represents cellular component, MF represents molecular function, BP represents biological process.

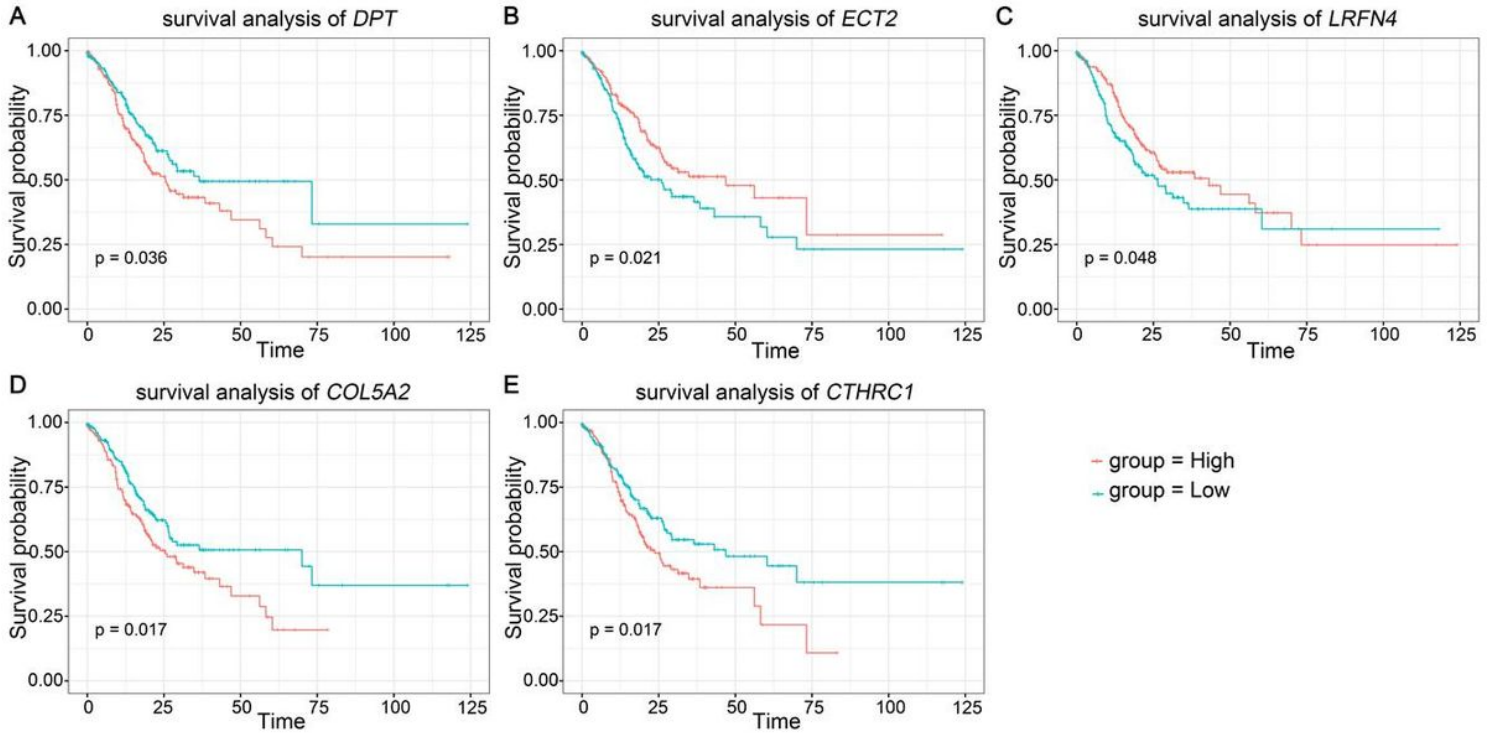

Figure 3

The prognostic value of key genes in the overall survival of Stomach adenocarcinoma (STAD) patients. (A) DPT. (B) ECT2. (C) LRFN4. (D) COL5A2. (E) CTHRC1. The red lines signified individuals with high expression of gene and blue lines with low expression.

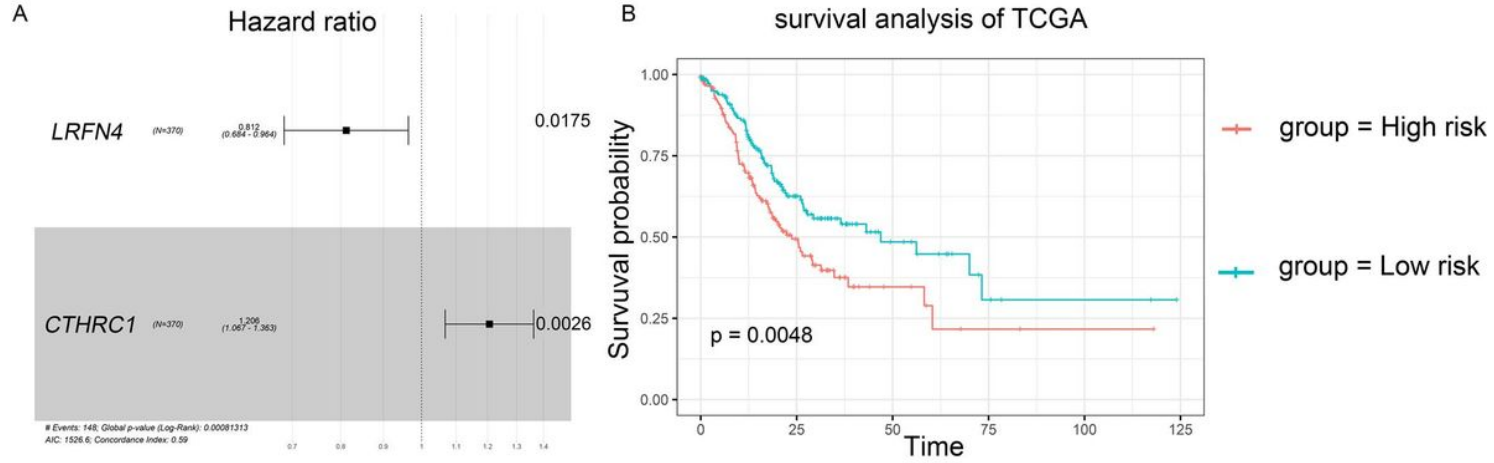

Figure 4

Prognostic value detection of LRFN4 and CTHRC1 via multivariate Cox regression analysis in patients with STAD of TCGA cohort. (A) Forest illustration showed result of multivariate Cox regression analysis. (B) Survival analysis of the high-risk group and the low-risk group.

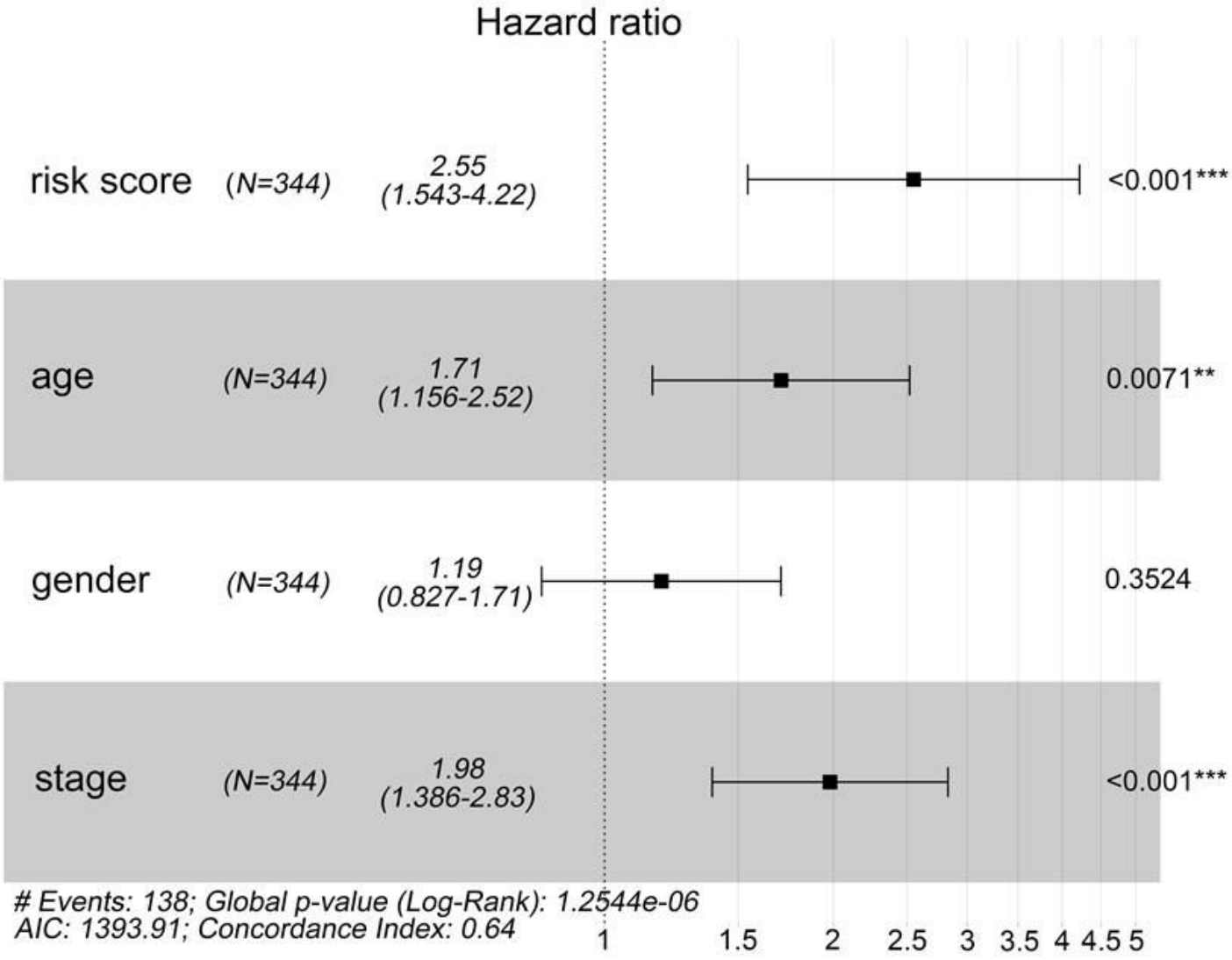

Figure 5

Multivariate Cox regression analysis of clinicopathologic factors and risk score for STAD in TCGA sets.

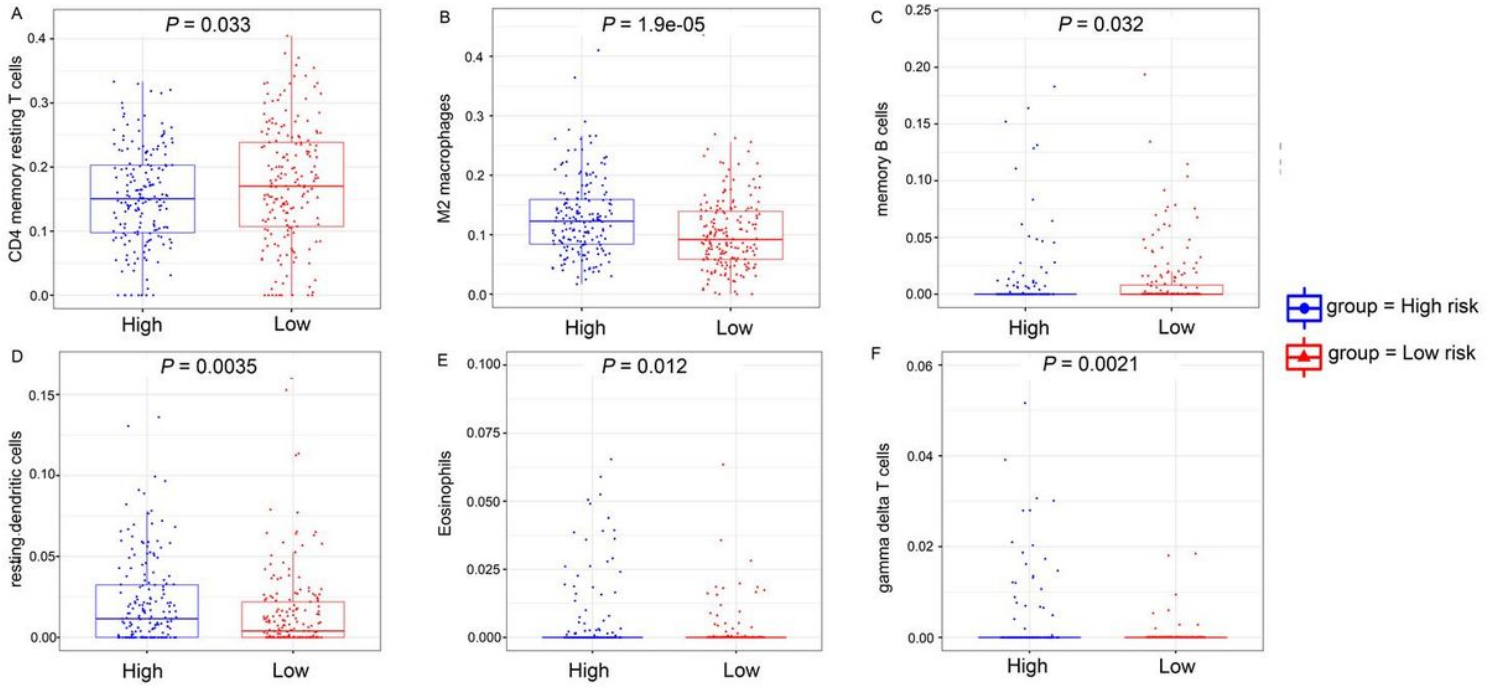

Figure 6

Multivariate Cox regression analysis of clinicopathologic factors and risk score for STAD in TCGA sets.

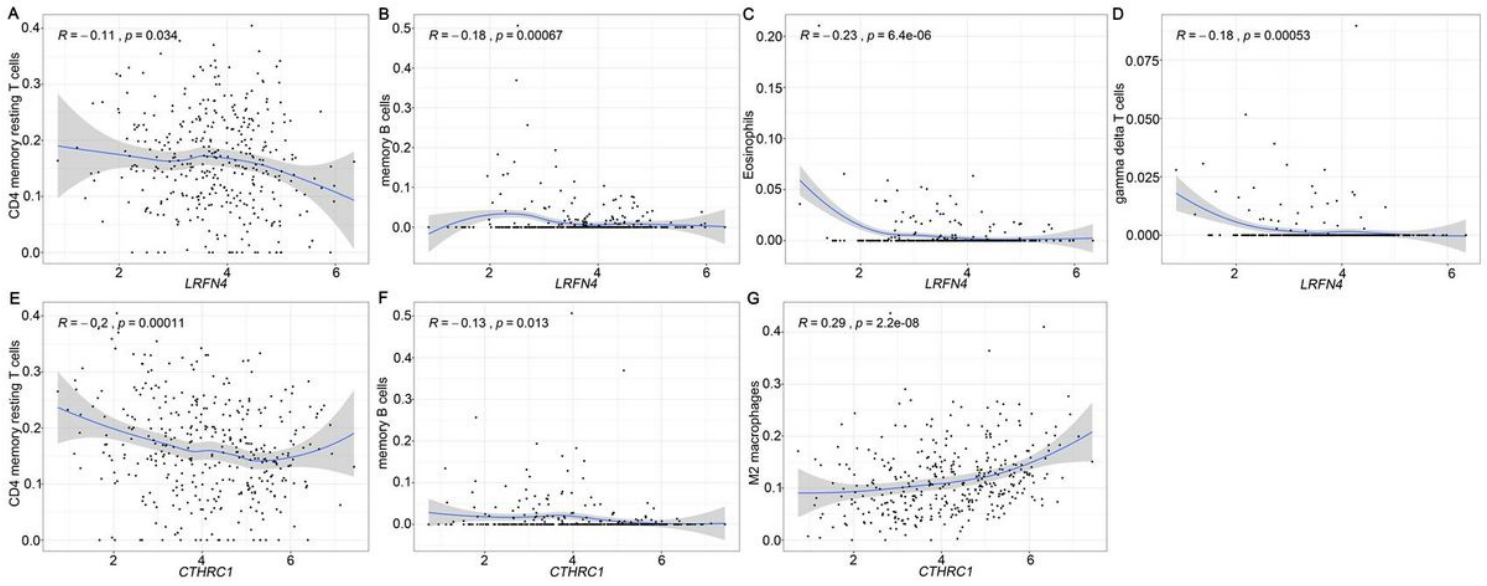

Figure 7

Correlations of mRNA expressions and human immune cell phenotypes. (A) CD4 memory resting T cells and LRFN4. (B) Memory B cells and LRFN4. (C) Eosinophils and LRFN4. (D) Gamma delta T cells and LRFN4. (E) CD4 memory resting T cells and CTHRC1. (F) Memory B cells and CTHRC1. (G) M2 macrophages and CTHRC1.

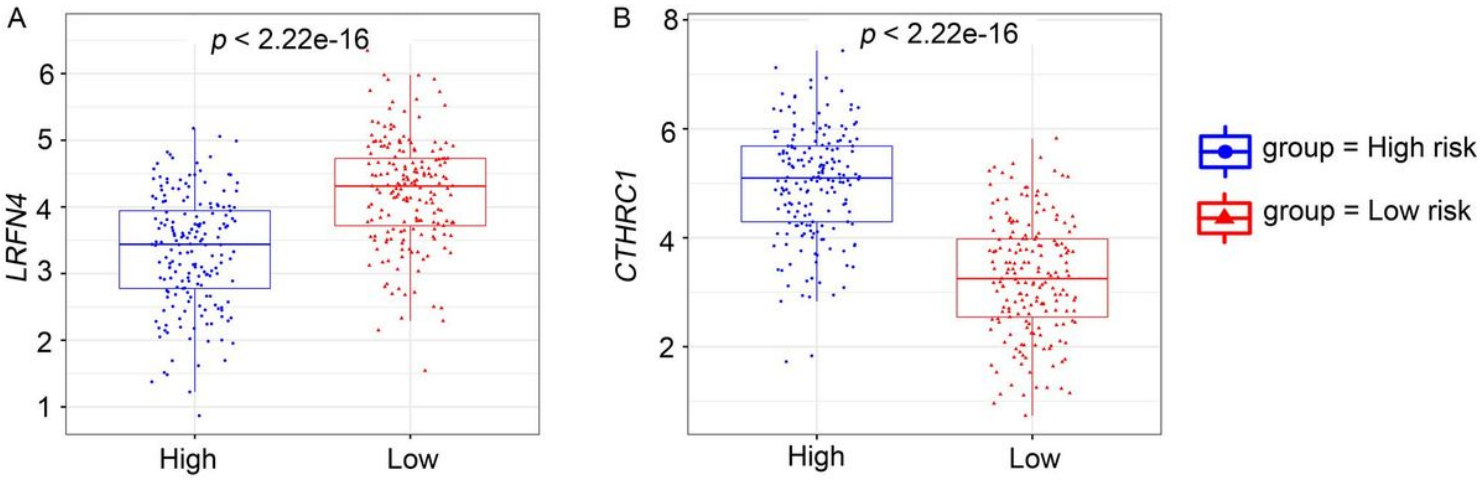

Figure 8

Gene expressions in TCGA dataset. (A) Expression of LRFN4 in the high- and low-risk groups in TCGA-STAD dataset. (B) Expression of CTHRC1 in the high- and low-risk groups in TCGA-STAD dataset.

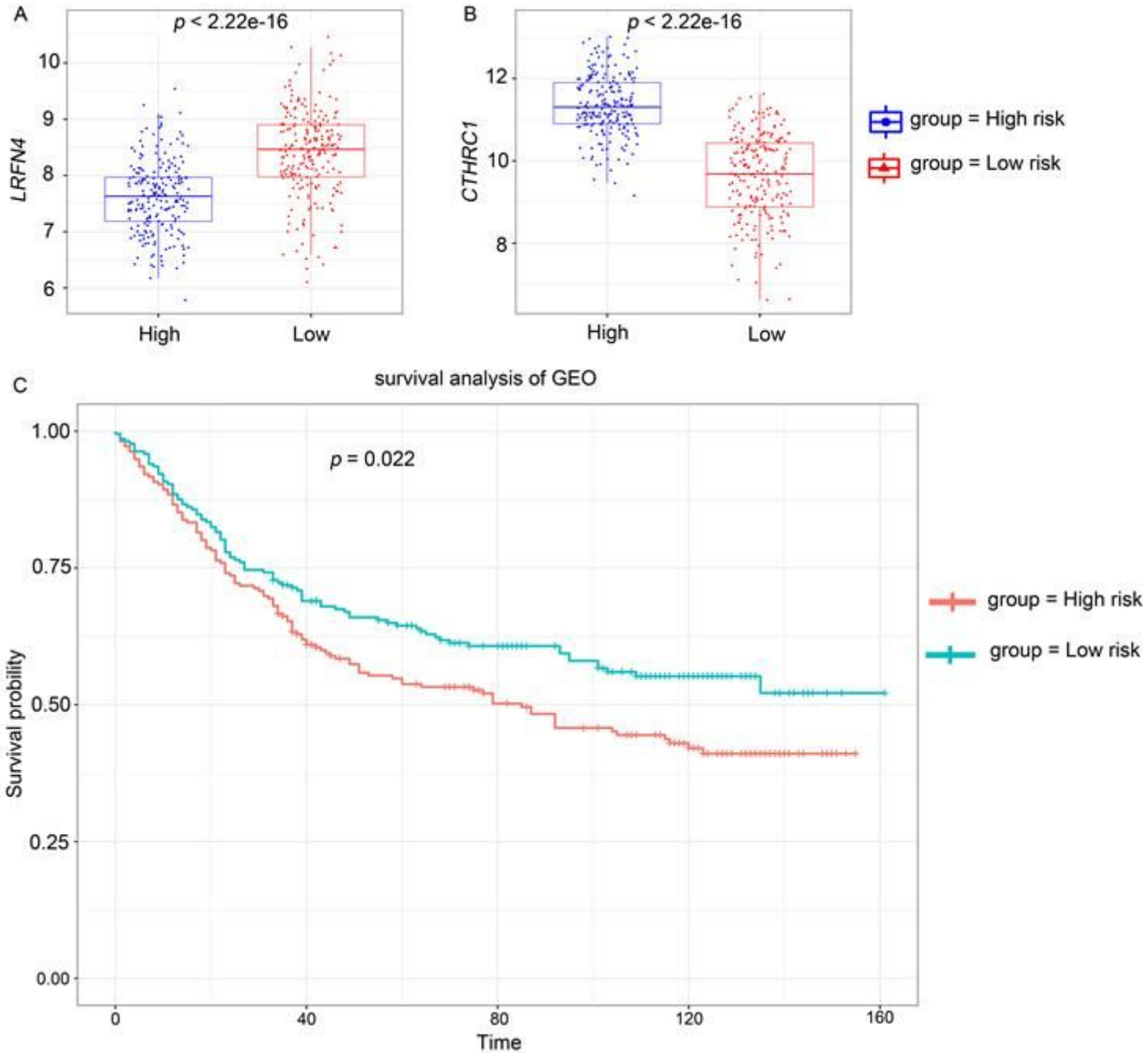

Figure 9

Evaluation of Prognostic Model for Over Survival in GEO dataset. (A) Expression of LRFN4 in the high- and low-risk groups in GEO dataset. (B) Expression of CTHRC1 in the high- and low-risk groups in GEO dataset. (C) Survival analysis of the high-risk group and the low-risk group in GEO dataset.